

## APPLIED RESEARCH

# Handy Kitchen Liquid Food Viscometer Using a DC Motor as Actuator and Sensor

Y. HAMADA<sup>1</sup>, (Member, IEEE), T. YOSHIDA<sup>2</sup>, Y. KURIHARA<sup>1</sup>, (Member, IEEE),  
AND K. WATANABE<sup>3</sup>, (Member, IEEE)

<sup>1</sup>Department of Science and Technology, Aoyama Gakuin University, Sagami-hara-shi 252-5258, Japan

<sup>2</sup>Department of Computer Science and Systems Engineering, Okayama Prefectural University, Okayama 719-1197, Japan

<sup>3</sup>Department of Science and Technology, Hosei University, Koganei-shi, Tokyo 184-8584, Japan

Corresponding author: Y. Kurihara (kurihara@ise.aoyama.ac.jp)

**ABSTRACT** Liquid food can likely cause accidental ingestion in patients with dysphagia. This study proposes a handheld stirrer-type rotational viscometer that can be used in the kitchen or at meals for dysphagia. A novel rotational viscometer is proposed considering that the rotation speed of the handheld stirrer is inversely proportional to the viscosity of the fluids to be stirred. We adopt the sensorless control strategy. We use a small brush-type DC motor, which functions as a rotary actuator and a rotational speed sensor to realize the proposed device. Because the proposed viscometer is used in the aforementioned fields, it must be compact, handy, simple in structure, and low-cost. We apply the proposed viscometer to fluids with viscosities ranging from 5000 to 54000 mPa·s for testing, using a cylindrical rotor with a length of 15 mm and diameter of 10 mm. The repeatability and linearity as a measurement instrument evaluated by the ASTM standards E3116-18 are less than 5% and 4% for the aforementioned fluids under the temperature of 11 °C, respectively. Because the thickness of liquid food is classified into only three categories (mildly, moderately, and extremely thick), the accuracy of this method is sufficient for the measurement.

**INDEX TERMS** Actuator, DC motor, thickness measurement of fluid food, viscometer.

## I. INTRODUCTION

Dysphagia is the difficulty in swallowing liquid foods that can cause aspiration and other respiratory problems [1], [2], [3]. Therefore, managing the thickening of liquid foods is crucial for the safety of patients with dysphagia. In swallowing care and rehabilitation, various methods to measure thickness have been proposed and standardized by considering viscosity. Thickness is a sensory quantity that humans perceive as “mouthfeel,” and fluids associated with thickening evaluation are predominantly non-Newtonian [4]. The thickness can be measured qualitatively by observing the ease of flow during the container tilting and fluid dripping from the spoon [4], [5]. The line spread test (LST) is a commonly used quantitative method [1], [6] and its procedure is as follows: (1) A flat sheet with a pie chart-shaped scale is placed on a horizontal surface and a cylindrical container with

an inner diameter of 30 mm is placed at the center of the scale. (2) The container is filled with 20 mL of the thickening fluid to be measured and allowed for 30 s. (3) The container is lifted vertically and the distances in six directions of the flowed-out fluid are measured after 30 s. The average distance was the LST value, measured in mm (or cm). The LST value is inversely proportional to the thickness and is categorized by a nominal scale as mildly, moderately, or extremely thick [7], [8].

Further, the thickness was measured quantitatively using viscometers [1], [4], [5]. The major types of viscometers are generally classified as a falling element, rotational, cone-and-plate, parallel-plate, pressure flow, capillary, and vibrational viscometers to determine the direct effect of the fluid on intended applications [9]. Conventional viscometers are based on the fluid dynamics of Newtonian fluids. Recently, viscometers have been innovated while inheriting the aforementioned conventional schemes. For example, as the falling element, a novel orbiting sphere viscometer for continuous

The associate editor coordinating the review of this manuscript and approving it for publication was Giambattista Gruosso<sup>1</sup>.

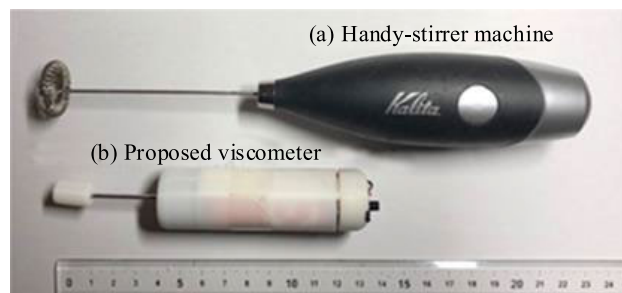
measurements was proposed [10]. For the rotational type, a new method using a stepping motor as an actuator was proposed [11]. For the pressure flow type, a novel microfluidic viscometer [12] and optical microfluidic co-flow viscometers were used to resolve problems related to optical measurements [13]. A capillary type was used as a novel measurement of the viscosity of water containing copper oxide nanoparticle suspensions [14]. A novel optical fiber probe comprising an air cavity with a small access hole was proposed for fluids in a hollow capillary tube [15]. For the vibration type, a novel simple silicon diaphragm vibration method, online vibration method based on the electromechanical impedance of a piezoelectric torsional transducer [17], and acoustic viscometer models [18] have been presented. A novel viscosity detection method based on a fiber Bragg grating longitudinally excited by an acoustic transducer has been presented [19]. The theoretical basis of these studies was Newtonian fluid dynamics. Thus, the application of these methods to non-Newtonian fluids is limited in terms of measurement accuracy.

Presently, thickness is classified using only the three aforementioned categories; thus, real-time measurement, rather than measurement accuracy, is required when cooking in kitchens and eating in hospital rooms and nursing homes. This is because the thickness and viscosity of liquid foods are influenced by the duration and temperature after cooking. It must be measured and managed immediately before eating.

As earlier mentioned, the LST method requires time and effort for measurement and the high-precision measurement of Newtonian fluids using viscometers is over-specified and inappropriate for thickness measurement. A thickness sensor must be convenient, inexpensive, and capable of providing results in real time.

This study proposes a handheld stirring-type rotational viscometer for liquid food used in the aforementioned fields. The development of a rotational handheld thickness measurement instrument requires a small rotational actuator and rotation sensor.

Generally, when constructing a system with the same performance in terms of reliability, durability, and cost, fewer components are preferred for simplicity. Determining an element with at least two functions is necessary for system realization. Sensorless control functions using this concept. For example, a motor exhibits the reversible property of a generator [20]. Studies on sensorless control using this reversibility are underway [20], [21], [22], [23]. In this study, because the frequency of noise generated when the feeding contact of a brush-type DC motor passes through the brush is proportional to the rotation speed [24], we propose a novel rotary viscosity meter that uses noise as a signal and functions as a DC motor and rotational speed sensor. Consequently, a small viscosity meter can be constructed with only three elements: a brush-type DC motor, driving power source, and processor, which can be used in the field, such as a handheld stirrer. The novelty of this proposal is based on the design



(a) Ordinary “Handy-stirrer machine” without viscosity measurement function

(b) “Proposed viscometer” is overall view of the proposed thickness measuring device with rotor

**FIGURE 1. Proposed hand-stirring-type rotational viscometer.**

philosophy of “the simple the best.” The measurement results obtained using the proposed method were evaluated using ASTM standard E3116-18 [25].

## II. ASSUMPTIONS AND ISSUES TO BE CONSIDERED

### A. PROPOSED DEVICE

An ordinary handheld stirring machine and the proposed handheld viscometer to compare the sizes of the two devices are shown in Figs 1 (a) and (b). When liquid food is stirred in a bowl using a handheld stirrer, the rotational speed of the stirrer decreased in proportion to the viscosity of the liquid food. This study focuses on this phenomenon and proposes a method to measure viscosity from the rotational speed of a stirrer driven by a brush-type DC motor. As described in Section III-C, a brush-type DC motor has two power supply contacts to supply the coils and switch the current in synchronization with the rotation. At switching, a high short-pulse noise owing to sparking appeared at the power supply terminal. The frequency of this pulse noise is proportional to the rotational speed of the motor. Using this pulse noise, the rotational speed can be measured without employing a dedicated sensor.

The rotational speed of the conventional rotational viscometer ranges from 6 to 60 rpm, whereas that of the proposed method ranges from 60 to 2200 rpm, which is considerably higher than that of the conventional viscometer. By decreasing the rotational speed, the fluid can be regarded as Newtonian by ignoring the centrifugal force acting on the fluid, which is the basis of the measurement principles of conventional rotational viscometers. In the proposed method, the rotational speed is high and the phenomenon that occurs is related to other phenomena, such as centrifugal force, dynamic friction, and static friction, which may influence the behavior of the fluid. Consequently, developing purely physical theoretical models is challenging. Thus, we adopt a physical theoretical model that includes several adjustable parameters, or a purely descriptive mathematical model that can be referred to as an empirical model.

**B. ASSUMPTIONS AND ISSUES TO BE CONSIDERED**

The following assumptions were considered to develop a theoretical model of the measurement principles and methods.

- (A1) The apparent viscosity is lower than the actual viscosity because of the peeling force of the fluid from the rotor caused by the centrifugal force.
- (A2) The resistance force received by the rotor from the fluid is influenced by dynamic and static friction and is provided by the resultant force of a force proportional to the rotational speed and a constant force that is independent of the rotational speed.

(A1) and (A2) are required to model the resistance force of the fluid with respect to the rotational motion of the rotor. The coefficients of the model were determined using calibration experiments. Based on the aforementioned assumptions, the following issues are addressed:

- (P1) The measurement principle is based on a theoretical model that represents the rotational speed of a rotor in a fluid attached to the shaft of a motor driven by constant-voltage rotation.
- (P2) An empirical model approximating the theoretical model in (P1) is determined.
- (P3) A rotational speed measurement strategy using a brush-type DC motor is presented.
- (P4) The measurement methods are validated based on the solutions of (P1), (P2), and (P3).

**III. VISCOSITY MEASUREMENT**

**A. THEORETICAL MODEL AND MEASUREMENT PRINCIPLE**

Here, (P1) was considered. First, the variables and constants were defined to build a theoretical model for the measurement principle.

- [DC Motor]
  - $B[T]$  : Magnetic flux density
  - $l[m]$  : Length of rotor coil
  - $R[\Omega]$  : Electrical resistance of the rotor coil
  - $J[Nm^2]$  : Inertial moment
  - $n$  : Number of poles
  - $E[V]$  : Applied voltage
  - $i[A]$  : Current
  - $t_n[s]$  : Noise generation interval between brushes in contact with power supply contacts
- [Rotor]
  - $r[m]$  : Radius
  - $L[m]$  : Length
  - $k[m]$  : Structural correction factor
  - $G[m^3]$  : Equivalent rotor volume
- [Fluid]
  - $\eta[Pa \cdot s]$  : Viscosity
  - $\eta_d[Pa \cdot s]$  : Apparent viscosity, defined as  $\eta - \eta_d$
  - $\omega_0[rad/s]$  : Static friction correction factor
  - $\omega[rad/s]$  : Rotational speed
  - $T_F[Nm]$  : Resistance torque

[Calibration coefficient for the descriptive mathematical model]

- $c_0[Pa \cdot s/\sqrt{V}]$  : Calibration coefficient
- $c_1[Pa \cdot s^2]$  : Calibration coefficient

From (A1) and (A2), the viscous reaction torque  $T_F[Nm]$  of the torque driven by the DC motor can be described as follows:

$$T_F = k(2\pi rL)(\eta - \eta_d)(\omega + \omega_0) \tag{1}$$

The rotational motion of the rotor connected to the rotating shaft of a DC motor is expressed as follows:

$$J \frac{d\omega(t)}{dt} + T_F(t) = Blri(t) \tag{2}$$

with

$$i(t) = \frac{E - Blr\omega(t)}{R} \tag{3}$$

When  $\frac{d\omega(t)}{dt} = 0$ , the aforementioned three equations yield the following equation.

$$k(2\pi rL)(\eta - \eta_d)(\omega + \omega_0) = Blr \frac{E - Blr\omega(t)}{R} \tag{4}$$

yielding

$$\begin{aligned} \eta &= \frac{Blr}{k(2\pi rL)R} \cdot \frac{E - Blr\omega(t)}{(\omega(t) + \omega_0)} + \eta_d \\ &= \frac{1}{GR} \cdot \frac{BlrE - (Blr)^2\omega(t)}{(\omega(t) + \omega_0)} + \eta_d \end{aligned} \tag{5}$$

From (5), the rate of decrease in viscosity  $\eta$  with respect to the rate of increase in rotational speed  $\omega(t)$  is proportional to  $(Blr)^2$ . Therefore, a DC motor with a high  $Blr$  should be used to increase the sensitivity of this type of viscometer. Equation (5) includes three adjustable unknown parameters,  $k$ ,  $\omega_0$ , and  $\eta_d$ . Because the term  $Blr / \{k(2\pi rL)R\}$  includes the unknown  $k$ , let  $k(2\pi rL) = G$ , as described in the third term of (5). The three parameters,  $G$ ,  $\omega_0$ , and  $\eta_d$  should be calibrated.

**B. EMPIRICAL MODEL**

Here, (P2) was considered. The blue curve in Fig. 2 shows the viscosity calculated using (5) for a small motor driven by a voltage of 4 V with parameters  $R = 102.3 \Omega$ ,  $Blr = 0.02376 \text{ Nm/A}$ ,  $E = 3 \text{ V}$ ,  $G = 9.52 \times 10^{-11} \text{ m}^3$ ,  $\eta_d = 1380 \text{ mPa} \cdot \text{s}$ , and  $\omega_0 = 125 \text{ rad/s}$ , which are the same as those in the experiment. As shown in Fig. 2, the calculated viscosity decreases with increasing rotational speed to fit the square-root function. Equation (5) can be approximated mathematically using the following square root function:

$$\eta = c_0\sqrt{E} - c_1\sqrt{\omega} \tag{6}$$

The viscosity calculated using (6) when  $E = 3 \text{ V}$ ,  $c_0 = 40700 \text{ Pa} \cdot \text{s}/\sqrt{V}$ , and  $c_1 = 6242 \text{ Pa} \cdot \text{s}^2$  is shown in red curve in Fig. 2. Curves (5) and (6) in Fig. 2 are in good agreement. The physical theoretical model in (5) can

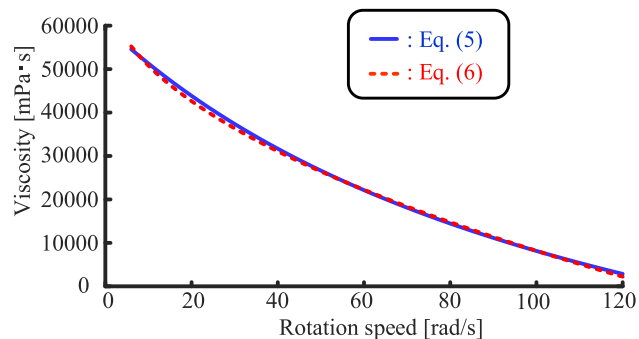


FIGURE 2. Calculated viscosity from motor rotational speed.

be used as a guideline to design a viscometer. By contrast, the mathematical and/or empirical model (6) can be used as a calibration function after manufacturing the viscometer device.

C. MEASUREMENT OF THE ROTATIONAL SPEED FROM BRUSH NOISE

(P3) is addressed accordingly. In a rotating n-pole-brushed DC motor, the brushes and power supply are in are connected with the current supplied to the motor coil. Because an n-pole motor has two power-supply contacts, the number of contacts per revolution is  $2n$ . When the contact conditions change, the amplitude varies, and the noise pulse waveform differs each time. However, despite these differences, noise was generated through sparking each time the brushes came into contact. These noise generation times can be captured by filtering the DC component from the power supply terminal using an HP filter, converting it to AC, and inputting the AC voltage into the comparator circuit. The output voltage of the comparator can be inputted to the processor and the noise generation time interval  $t_n$  can be calculated. However, suppose the comparator fails to count the noise occurrence. In that case, the time interval is a double or integer multiple of other time intervals and the processor can correct this failure. The rotational speed  $\omega$  is calculated from time interval  $t_n$  as follows:

$$\omega = \frac{2\pi}{2nt_n} = \frac{\pi}{nt_n} \text{ [rad/s]} \tag{7}$$

IV. EXPERIMENTAL VALIDATION

Here, (P4) is treated experimentally.

A. EXPERIMENTAL SETUP

The experimental setup is shown in Fig. 3. A reference rotational viscometer (NDJ-1) with four rotors to measure different ranges of viscosities and the experimental setup for the proposed method using a DC motor are shown in the figures on the left and right, respectively. Viscosity was measured by pouring the test fluid into a 166 mL acrylic cylindrical container with an inner diameter of 46 mm and length of 100 mm using the method specified by the reference rotational viscometer. Rotor #4 shown in Fig. 3 was used

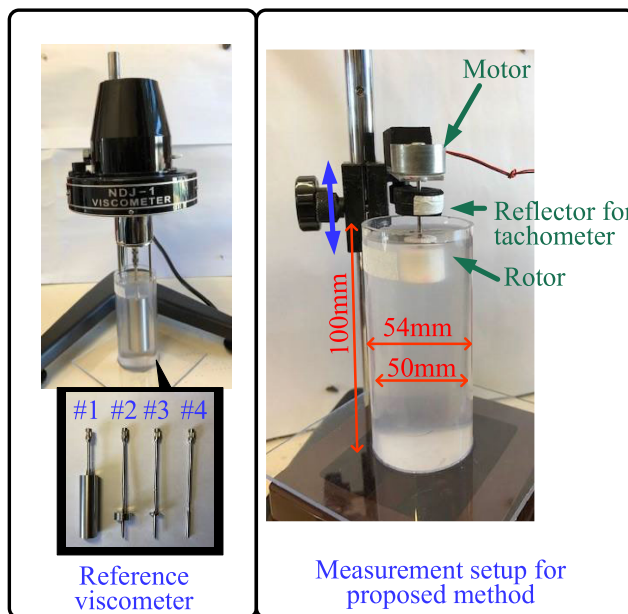


FIGURE 3. Viscosity measurements.

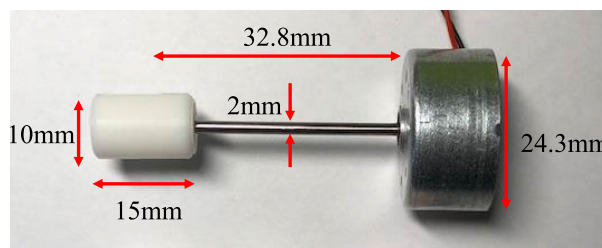


FIGURE 4. Viscosity measurements.

when a high viscosity as the reference fluid was measured with a reference viscometer and rotor #1 was used during low viscosity measurements. The rotational speed was set to 6 rpm. Fluids (400 mL) with different viscosities were prepared using water, sugar, and different amounts of xanthan gum as thickening agents. The 34 reference fluids with viscosities ranging from 5000 mPa·s to 54000 mPa·s were prepared to evaluate the thickness. These are the high-risk factors for dysphagia. The triode DC motor (uxcell-DC motor) for the toy boat model is shown in Fig. 4. The coil resistance was 94  $\Omega$ , self-inductance was 61.8 mH, and  $Blr = 0.02376$  Nm/A. The specified voltage was 4 V and the specified rotational speed was 2000 rpm. An 8.3  $\Omega$  resistor was connected in series to measure the current. The  $Blr$  values of the other two motors were measured; the  $Blr$  of this motor was at its maximum. Additionally, the long shaft of the motor shown in Fig. 4 is desirable for the application in this study. A cylindrical rotor with a diameter of 10 mm and a length of 15 mm was used. The rotational speed was measured using a noncontact tachometer (GM8905) and the noise generation interval data were measured and stored in a memory scope (RIGOL DS1054) for use in the method based on (7). The rotational speed was measured using a noncontact tachometer



after validating that the measurement results were nearly identical.

**B. MEASUREMENT OF ROTATIONAL SPEED BY BRUSH NOISE**

The solution to (P3) was validated experimentally. The circuit that captured the brush noise appearing in the power supply, output voltage, and average period, frequency, and rotational speed obtained from the noise generation time interval are shown in Fig 5 (a), (b), and (c), respectively. The error between the measurement using the noncontact tachometer and the estimated rotational speed was 0.02%. The rotational speed obtained from the brush noise generation time interval was approximately the same as that measured using a non-contact tachometer. A noise filter is necessary when driving a processor using the same power supply.

Generally, DC motor temperatures ranged from 25°C to 70°C, which is room temperature. Within this range, the effects of temperature on the DC motor were minor and performance-related changes were limited. The basic component of the proposed viscometer is a DC motor used at room temperature in environments, such as kitchens and hospital rooms. Therefore, the effects of the temperature were insignificant.

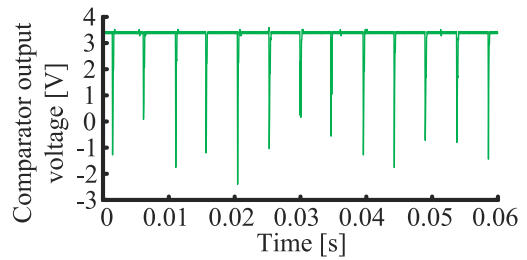
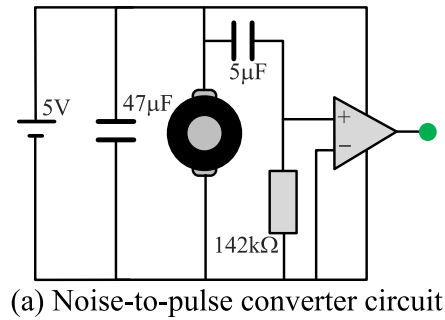
**C. VISCOSITY MEASUREMENT OF HIGH-VISCOSITY FLUID**

The validity of the solutions for (P1) and (P2) in the aforementioned reference fluids are validated here. The rotor of the viscometer (NDJ-1) used to measure the reference fluids was #4 in Fig. 3, the rotational speed was 6 rpm, and the fluid and room temperatures were 11 °C. Next, the rotational speed of the proposed DC motor was measured using a noncontact tachometer.

The viscosities of the viscous liquids measured using a standard viscometer were treated as a reference; thus, the viscosities were estimated using the proposed device. The results are shown in Figs. 6 and 7.

The rotational speed of the motor, when the rotor was placed in the fluid, is shown in Fig. 6 (a). From Fig. 6 (a), the rate of decrease in rotational speed with respect to the rate of increase in viscosity was low when the viscosity was less than 7000 mPa·s and increased when the viscosity exceeded 7000 mPa·s. The viscosities and estimation errors estimated using (5) under supply voltages of 3, 4, and 5 V are shown in Figs. 6 (b) and (c). The three parameters in (5) were optimally fitted to the data shown in Fig. 6 (a) and their values are listed in the left-hand column of Table 1. The measurement error for each applied voltage was briefly evaluated. The standard deviations of the measurement errors were 21.8, 8.74, and 8.78% for 3, 4, and 5 V supply voltages, respectively. Therefore, high-voltage power supplies provide accurate measurements.

The viscosity estimated using (6) is shown in Fig. 7 (a). The measurement errors from direct measurements for 3-, 4, and 5 V power supply voltages are shown in Fig. 7 (b). The right column of Table 1 lists the parameters that optimally



	Estimated	Measured	Error	Error [%]
Average period [s]	0.02855	0.02854	$-6 \times 10^{-6}$	-0.02017
Frequency [Hz]	35.0263	35.0333	0.00706	0.020163
Rotational speed [rpm]	2101.58	2102	0.42382	0.020163

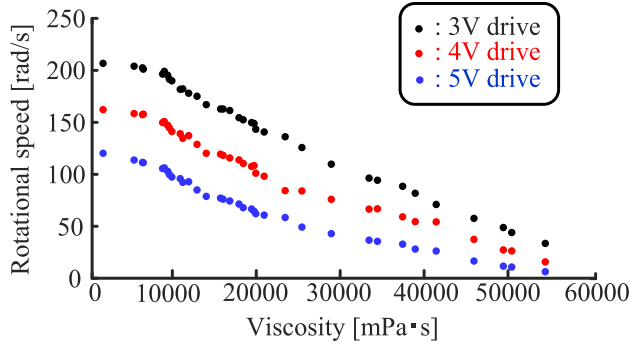
(c) Directly measured and estimated using (7)

**FIGURE 5. Rotational speed estimation.**

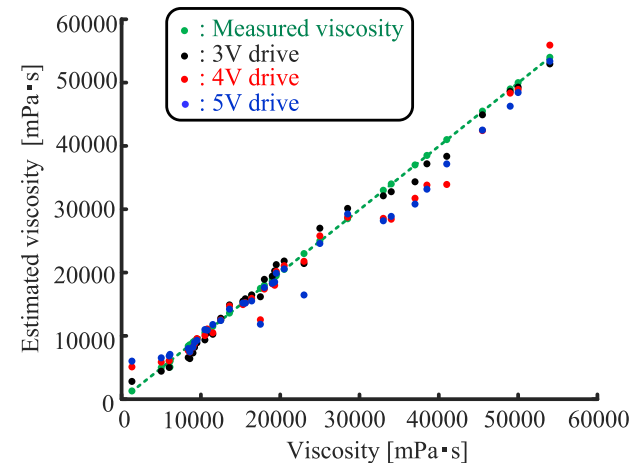
fit (6) for the data shown in Fig. 6 (a). Additionally, the measurement error for each applied voltage was re-evaluated. The standard deviations of the estimation error were 14.5, 10.4, and 10.1% for the 3, 4, and 5 V power supply voltages, respectively. For (5) and (6), the standard deviation of the error increased when the motor was driven at a low voltage of 3 V because the motor did not operate stably at 3 V, considering the specified power supply voltage of the motor was 4 V. The standard deviation of the error when the motor was driven at 4 and 5 V was approximately 8.4% of the estimated viscosity in (5), whereas the estimation error of (6) was approximately 10%. Thus, the method using (5) was slightly better than that using (6) in terms of accuracy and physical interpretation. However, the number of calibration parameters in (5) was three, and that in (6) was two, indicating that (6) was better in terms of ease of calibration. Based on the error analysis for the voltage in Fig. 7, the errors in the 4 V and 5 V power supplies were small.

**D. EVALUATION OF THE ESTIMATION OF THE PROPOSED METHOD AS A MEASURING INSTRUMENT**

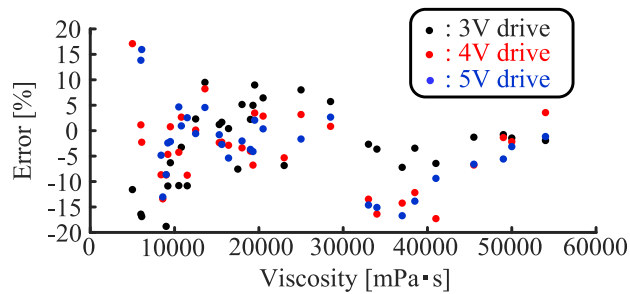
The results shown in Figs. 6 and 7 from theoretical model (5) and empirical model (6) were evaluated as models for measuring instrument by ASTM E3116-18. The viscosity range



(a) Viscosity vs. rotational speed



(b) Viscosity estimated by (5)



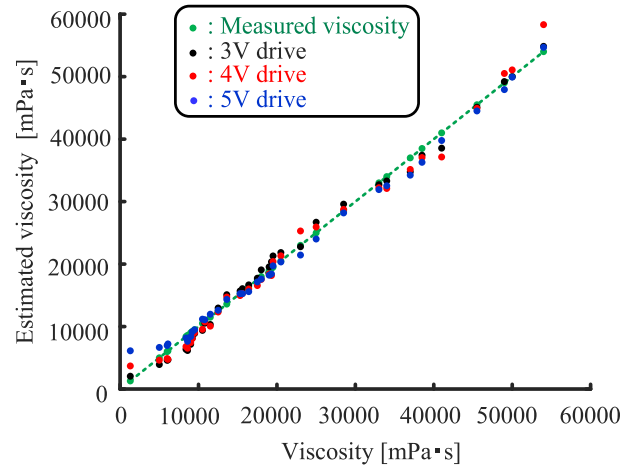
(c) Estimation error

**FIGURE 6.** Estimation of viscosity from rotational speed for different supply voltages using (5).

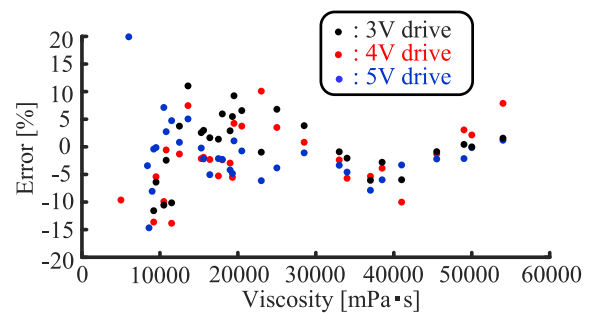
and temperature required for the ASTM evaluation were 5000–54000 mPa·s and 11 °C, respectively. The reference and measurement data are shown in Figs. 6 and 7, respectively. Table 2 lists the results. Here, the evaluation parameters are defined, as follows.

- $re$  [%]: Repeatability
- $DL$  [mPa·s]: Detection limit
- $QL$  [mPa·s]: Quantitation limit
- $Li$  [%]: Viscosity linearity
- $Bias$  [mPa·s]: Viscosity bias

The repeatability  $re$  was less than 5% for all conditions. The limit of detection  $DL$  and limit of quantitation  $QL$  increased with increasing voltage for the theoretical and



(a) Viscosity estimated using (6)



(b) Estimation error

**FIGURE 7.** Estimation of viscosity from rotational speed for different supply voltages using (6).

**TABLE 1.** Parameters in (5) and (6).

$E$ [V]	Parameters in (5)			Parameters in (6)	
	$G$ [m <sup>3</sup> ]	$\eta_d$ [mPa·s]	$\omega_0$ [rad/sec]	$c_0$ [Pa·s/ $\sqrt{V}$ ]	$c_1$ [Pa·s <sup>2</sup> ]
3	$9.52 \times 10^{-11}$	125	1380	40700	6242
4	$9.09 \times 10^{-11}$	150	3907	41500	6227
5	$6.45 \times 10^{-11}$	250	5318	77809	5655

empirical models. The linearity  $Li$  was less than 4% for the theoretical model and within 3% for the empirical model.  $Li$  was the lowest for the theoretical and empirical models when the motor was driven at 4 V, the rated voltage of the motor. The  $Bias$  value at 5 V was twice that at 3 and 4 V in the theoretical model. In the empirical model, the value at 5 V was positive, whereas those at 3 and 4 V were negative. Because the thickness was evaluated based on three categories on a nominal scale, these results sufficiently apply to fluid thickening evaluations. Notably, from the perspective of standard error deviations, the results of the three categories were 14.5%, 10.4%, and 10.1%. However, in the evaluation using the ASTM E3116-18 method as shown in Table 2, the repeatability and linearity evaluated using the method were less than 5% and 4%, respectively.

TABLE 2. Evaluation result by ASTM standard E3116-18.

Feeding voltage	Equation (5) Theoretical model					Equation (6) Empirical model				
	<i>re</i> [%]	<i>DL</i> [mPa·s]	<i>QL</i> [mPa·s]	<i>Li</i> [%]	<i>Bias</i> [mPa·s]	<i>re</i> [%]	<i>DL</i> [mPa·s]	<i>QL</i> [mPa·s]	<i>Li</i> [%]	<i>Bias</i> [mPa·s]
3 [V]	4.37	637	1930	3.83	737.61	4.71	610	1849	2.99	-230.19
4 [V]	4.52	873	2647	0.09	731.10	4.52	689	2089	0.20	-913.56
5 [V]	4.36	938	2842	0.91	1448.54	4.22	927	2809	2.25	1006.78

V. RESULTS AND CONSIDERATIONS

The error in the motor’s rotational speed determined from the high short pulse noise generated by the brush-type DC motor during rotation was 0.02016%. This was sufficient precision to measure the rotational speed of the rotational viscometer. We investigated the relationship between the rotational speed and viscosity of 34 test fluids with viscosities ranging from 5000 to 54000 mPa·s using a standard rotational viscometer and a single rotor with a diameter of 10 mm and length of 15 mm and determined the theoretical and experimental calibration formulas. The coefficients in these equations vary depending on the voltage applied to the DC motor.

Regarding the simple error estimation for the 3, 4, and 5 V supply voltage differences, the standard deviations of the measurement errors of the theoretical model method were 21.8, 8.74, and 8.78%, respectively. For the empirical model method, the standard deviations were 14.5, 10.4, and 10.1%, respectively. The measurement results were evaluated using the ASTM E3116-18 method. The repeatability and linearity evaluated using this method were less than 5% and 4%, respectively, for theoretical and empirical model methods.

We compared the characteristics of viscosity measurements using the proposed and conventional methods. The standard viscometer was a rotary method, whereas the standard for the thickness measurement was the LST method. Therefore, the viscometer used in the experiments was compared with standard LST sheet methods. The LST method was used to measure the thickness and did not directly output the viscosity. However, thickness and viscosity are related [1], which can be expressed by an exponential function as follows:

$$Viscosity = Ae^{-B(LST\ value - C)}$$

From the fluid thickness and viscosity measured under the same conditions, we optimally estimated the coefficient of viscosity from the thickness using an exponential function comprising three coefficients, *A*, *B* and *C*. Thus, the viscosity was estimated from the thickness using the LST value. The three coefficients were obtained as *A* = 45000mPa · s, *B* = 1.16cm<sup>-1</sup>, and *C* = 2cm. From the estimated viscosity, we obtained the error similarly to evaluate the proposed method. The LST value vs. viscosity, measured, and estimated viscosities are shown in Fig. 8. The standard deviation of the estimated error was 19.7 mPa·s.

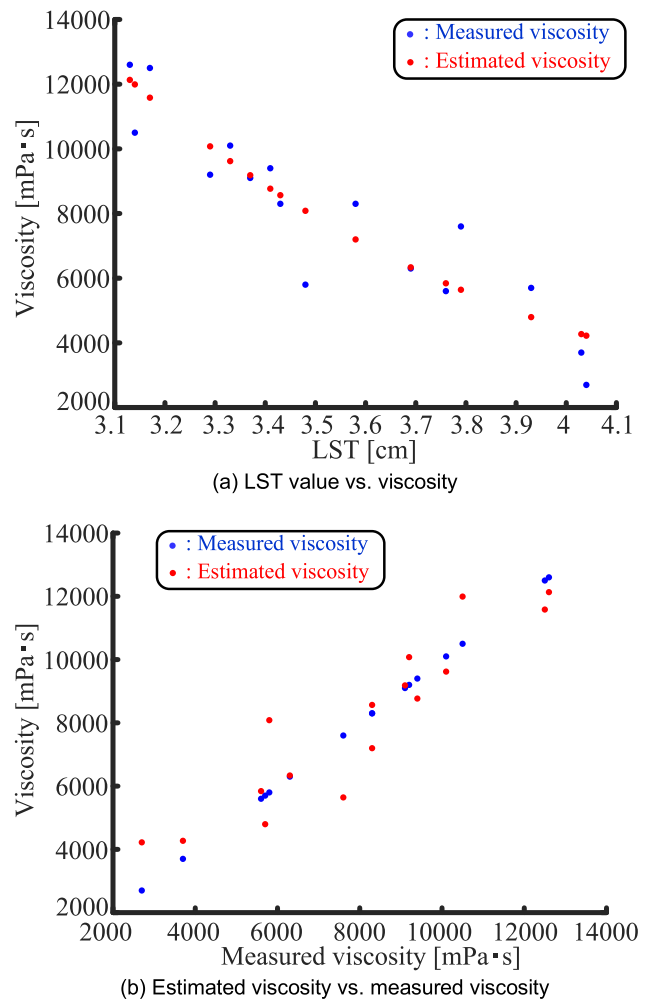


FIGURE 8. Estimated viscosity from LST value.

A comparison of the proposed method with the conventional viscometer and LST methods is shown in Table 3. The proposed method is advantageous in that it has a wide measurement range without rotor replacement, online on-site measurement, simple structure, no skill requirement in operation, and is inexpensive compared with other methods. The error was half the viscosity estimated from the LST value. However, the error was twice that of the viscometer. This method is sufficiently accurate for use as a thickness measurement method for liquid foods.

TABLE 3. Comparison with other methods.

	Proposed Method	NDJ-1 Rotary Viscometer	LST
Range [mPa · s]	100-54,000	10-100,000	30-12,600
Error [%]	±10.1%	±5%	±19.7%
System components	DC motor, battery, and processor  (Simple)	Power source, synchronous motor, pointer, scale disk, hairspring, and rotor (complicated and fine)	LST sheet and ring  (Simple)
Online real time / Offline processing	Online real-time On-site measurement	Off-line lab-measurements	Off-line On-site measurement
Rotor replacement by viscosity	Not required	Required	Not required
Skill of operation	Not required	Required	Required
Cost	Inexpensive	Expensive	Inexpensive

## VI. CONCLUSION

This study proposed a novel thickness measurement instrument and/or viscometer for liquid foods. This instrument is simple, handy, inexpensive, and can be classified as a rotational viscometer.

The velocity of the battery-powered hand stirrer decreased when the stirring rotor was rotated in a highly viscous fluid. This study focused on this phenomenon and examined the feasibility of the viscometer in measuring the thickness of liquid foods. The results for (P1), (P2), (P3), and (P4) are summarized as follows:

For (P1), a three-parameter theoretical model for viscosity in conjunction with the DC motor was built, as shown in (5).

For (P2), a two-parameter empirical model (6), which was an approximation of the theoretical model, was presented.

For (P3), a method to measure the rotational speed of the DC motor was developed.

For (P4), the results for (P1), (P2), and (P3) were validated through experiments. The repeatability and linearity of viscosity measurements were less than 5% and 4%, respectively. Because the thickness of liquid food was evaluated using only three nominal categories, the accuracy of this method was sufficient for thickness measurement. Finally, this method only stirred liquid foods with a small rotor and is unlikely to influence the food quality.

Compared with the rotational viscometer and LST methods, the proposed method has a wide measurement range without rotor replacement, online on-site measurement, simple structure, no skill requirement for operation, and is inexpensive.

## REFERENCES

- [1] S.-G. Kim, W. Yoo, and B. Yoo, "Relationship between apparent viscosity and line-spread test measurement of thickened fruit juices prepared with a xanthan gum-based thickener," *Preventive Nutrition Food Sci.*, vol. 19, no. 3, pp. 242–245, Sep. 2014, doi: [10.3746/pnf.2014.19.3.242](https://doi.org/10.3746/pnf.2014.19.3.242).
- [2] T. Suzuki, R. Saito, N. Kitada, T. Koike, S. Maki, Y. Michiwaki, G. Nishimura, H. Niwa, and Y. Yamada, "Aspiration risk detection using oral administration of fluorescent food—Preliminary experiments using meat phantoms," in *Proc. IEEE Int. Conf. Cyborg Bionic Syst. (CBS)*, Oct. 2017, p. 2428, doi: [10.1109/CBS.2017.8266108](https://doi.org/10.1109/CBS.2017.8266108).
- [3] M. Nii, S. Okajima, R. Sakashita, M. Hamada, and S. Kobashi, "Tongue movement classification in chewing and swallowing using electromyography," in *Proc. 6th Int. Conf. Informat., Electron. Vis. 7th Int. Symp. Comput. Med. Health Technol. (ICIEV-ISCMT)*, Sep. 2017, pp. 1–6, doi: [10.1109/ICIEV.2017.8338594](https://doi.org/10.1109/ICIEV.2017.8338594).
- [4] A. Deblais, E. D. Hollander, C. Boucon, A. E. Blok, B. Veltkamp, P. Voudouris, P. Versluis, H.-J. Kim, M. Mellema, M. Stieger, D. Bonn, and K. P. Velikov, "Predicting thickness perception of liquid food products from their non-Newtonian rheology," *Nature Commun.*, vol. 12, no. 1, p. 6328, Nov. 2021.
- [5] Y. Iwasaki and H. Ogoshi, "Relation between non-oral sensory evaluations, oral sensory evaluation, and viscosity of commercial thickening agents—Consideration difference shear rate dependence," *J. Soc. Rheol. Jpn.*, vol. 42, no. 3, 2013, Art. no. 169175.
- [6] B. Adeleye and C. Rachal, "Comparison of the rheological properties of ready-to-serve and powdered instant food-thickened beverages at different temperatures for dysphagic patients," *J. Amer. Dietetic Assoc.*, vol. 107, no. 7, pp. 1176–1182, Jul. 2007.
- [7] E. Watanabe, Y. Yamagata, J. Fujitani, I. Fujishima, K. Takahashi, R. Uyama, H. Ogoshi, A. Kojo, H. Maeda, K. Ueda, and J. Kayashita, "The criteria of thickened liquid for dysphagia management in Japan," *Dysphagia*, vol. 33, no. 1, pp. 26–32, Feb. 2018, doi: [10.1007/s00455-017-9827-x](https://doi.org/10.1007/s00455-017-9827-x).
- [8] M. A. Nicosia and J. Robbins, "The usefulness of the line spread test as a measure of liquid consistency," *Dysphagia*, vol. 22, no. 4, pp. 306–311, Oct. 2007, doi: [10.1007/s00455-007-9086-3](https://doi.org/10.1007/s00455-007-9086-3).
- [9] S. A. Dyer, *Survey of Instrumentations and Measurement*. Hoboken, NJ, USA: Wiley, 2001.
- [10] S. Clara, H. Antlinger, and B. Jakoby, "Theoretical analysis and simulation studies of the orbiting sphere viscometer," *IEEE Sensors J.*, vol. 14, no. 10, pp. 3669–3676, Oct. 2014, doi: [10.1109/JSEN.2014.2330875](https://doi.org/10.1109/JSEN.2014.2330875).
- [11] S. E. de Lucena and W. Kaiser, "Stepping-motor-driven constant-shear-rate rotating viscometer," *IEEE Trans. Instrum. Meas.*, vol. 57, no. 7, pp. 1338–1343, Jul. 2008, doi: [10.1109/TIM.2008.917170](https://doi.org/10.1109/TIM.2008.917170).
- [12] T.-A. Lee, W.-H. Liao, and Y.-C. Tung, "Fully disposable and optically transparent microfluidic viscometer based on electrofluidic pressure sensor," in *Proc. 19th Int. Conf. Solid-State Sensors, Actuat. Microsystems*, Jun. 2017, pp. 579–582, doi: [10.1109/TRANSDUCERS.2017.7994115](https://doi.org/10.1109/TRANSDUCERS.2017.7994115).
- [13] M. A. Hintermüller, C. Offenzeller, and B. Jakoby, "A microfluidic viscometer with capacitive readout using screen-printed electrodes," *IEEE Sensors J.*, vol. 21, no. 3, pp. 2565–2572, Feb. 2021, doi: [10.1109/JSEN.2020.3024837](https://doi.org/10.1109/JSEN.2020.3024837).



- [14] J. Li, Z. Li, and B. Wang, "Experimental viscosity measurements for copper oxide nanoparticle suspensions," *Tsinghua Sci. Technol.*, vol. 7, no. 2, pp. 198–201, Apr. 2002.
- [15] A. D. Gomes, J. Kobelke, J. Bierlich, K. Schuster, H. Bartelt, and O. Frazao, "Optical fiber probe viscometer based on hollow capillary tube," *J. Lightw. Technol.*, vol. 37, no. 18, pp. 4456–4461, Sep. 15, 2019, doi: [10.1109/JLT.2019.2890953](https://doi.org/10.1109/JLT.2019.2890953).
- [16] I. Puchades and L. F. Fuller, "A thermally actuated microelectromechanical (MEMS) device for measuring viscosity," *J. Microelectromech. Syst.*, vol. 20, no. 3, pp. 601–608, Jun. 2011, doi: [10.1109/JMEMS.2011.2127447](https://doi.org/10.1109/JMEMS.2011.2127447).
- [17] G. Wang and F. Li, "An online viscosity measurement method based on the electromechanical impedance of a piezoelectric torsional transducer," *IEEE Sensors J.*, vol. 18, no. 21, pp. 8781–8788, Nov. 2018, doi: [10.1109/JSEN.2018.2867102](https://doi.org/10.1109/JSEN.2018.2867102).
- [18] Y. Ai and R. A. Lange, "Theoretical analyses and numerical simulations of the torsional mode for two acoustic viscometers with preliminary experimental tests," *IEEE Trans. Ultrason., Ferroelectr., Freq. Control*, vol. 55, no. 3, pp. 648–658, Mar. 2008, doi: [10.1109/TUFFC.2008.689](https://doi.org/10.1109/TUFFC.2008.689).
- [19] H. Qian, L.-Y. Shao, W. Zhang, X. Zhang, H. He, B. Luo, W. Pan, X. Zou, and L. Yan, "Fiber-optic viscometer with all-fiber acousto-optic superlattice modulated structure," *J. Lightw. Technol.*, vol. 36, no. 18, pp. 4123–4128, Sep. 15, 2018, doi: [10.1109/JLT.2018.2859239](https://doi.org/10.1109/JLT.2018.2859239).
- [20] S. Oh, K. Kong, and Y. Hori, "Design and analysis of force-sensor-less power-assist control," *IEEE Trans. Ind. Electron.*, vol. 61, no. 2, pp. 985–993, Feb. 2014, doi: [10.1109/TIE.2013.2270214](https://doi.org/10.1109/TIE.2013.2270214).
- [21] Y. Li, W. Li, L. Guo, N. Jin, and F. Lu, "Current sensor-less virtual synchronous generator model predictive control based on sliding mode observer," *IEEE Access*, vol. 9, pp. 17898–17908, 2021, doi: [10.1109/ACCESS.2021.3053587](https://doi.org/10.1109/ACCESS.2021.3053587).
- [22] M. A. Khoshhava, H. A. Zarchi, and G. A. Markadeh, "Sensor-less speed and flux control of dual stator winding induction motors based on super twisting sliding mode control," *IEEE Trans. Energy Convers.*, vol. 36, no. 4, pp. 3231–3240, Dec. 2021, doi: [10.1109/TEC.2021.3077829](https://doi.org/10.1109/TEC.2021.3077829).
- [23] A. Bhowate, M. V. Aware, and S. Sharma, "Speed sensor-less predictive torque control for five-phase induction motor drive using synthetic voltage vectors," *IEEE J. Emerg. Sel. Topics Power Electron.*, vol. 9, no. 3, pp. 2698–2709, Jun. 2021, doi: [10.1109/JESTPE.2020.3016335](https://doi.org/10.1109/JESTPE.2020.3016335).
- [24] R. J. Hamilton, "DC motor brush life," *IEEE Trans. Ind. Appl.*, vol. 36, no. 6, pp. 1682–1687, Nov./Dec. 2000, doi: [10.1109/28.887222](https://doi.org/10.1109/28.887222).
- [25] *Standard Test Method for Viscosity Measurement Validation of Rotational Viscometers*, ASTM Standards E3116-18, 2018.

**Y. HAMADA** (Member, IEEE) received the B.S., M.S., and Ph.D. degrees in engineering from Chuo University, Japan, in 2008, 2010, and 2017, respectively.

From 2018 to 2020, she was an Assistant Professor with Chuo University. Since 2020, she has been an Assistant Professor with the Industrial and Systems Engineering Department, Aoyama Gakuin University. Her research interests include the modeling of communication processes and analysis of decision-making processes.

Dr. Hamada is a member of the Japan Society of Kansei Engineering and the Japanese Cognitive Science Society.

**T. YOSHIDA** received the M.E. and Ph.D. degrees from Hosei University, Tokyo, in 2015 and 2018, respectively. He has been an Assistant Professor with Okayama Prefectural University, since 2018. His research interests include systems engineering, sensing methods, biosensing, and system information engineering. He is a member of the *Unmanned Vehicle Systems* and the *Intelligent Informatics*.

**Y. KURIHARA** (Member, IEEE) received the M.E. and Ph.D. degrees from Hosei University, Tokyo, in 2003 and 2009, respectively.

He joined Hitachi Software Engineering, Ltd., in 2003. From 2009 to 2012, he was an Assistant Professor with Seikei University. From 2013 to 2018, he was an Associate Professor with Aoyama Gakuin University, where he has been a Professor, since 2019. He is the author of five books, more than 80 journal articles, more than 100 international publications in conference proceedings, and he holds four patents. His research interests include systems engineering, sensing methods, biosensing, and system information engineering.

Prof. Kurihara is a member of the Japanese Society for Medical and Biological Engineering, the Society of Instrument and Control Engineers, Electrical Engineers of Japan, and the Japan Society for Fuzzy Theory and Intelligent Informatics.

**K. WATANABE** (Member, IEEE) received the M.E. and Ph.D. degrees in engineering from the Tokyo Institute of Technology, in 1968 and 1971, respectively, and the Ph.D. degree in medical science from Tokyo Medical and Dental University, in 2011.

From 1969 to 1971, he was a Research Assistant with the Faculty of Engineering, Hosei University. From 1971 to 1974, he was a Lecturer. From 1974 to 1984, he was an Associate Professor. From 1985 to 2015, he was a Professor. From 1980 to 1981, he was a Visiting Associate Professor with Oakland University, Rochester, MI, USA. From 1981 to 1982, he was a Research Associate with The University of Texas at Austin, Austin, TX, USA. He is currently a Professor Emeritus with Hosei University. In the industrial fields, he acts as an authorized PE. He is a Chief Researcher on several projects conducted by the Ministry of Economy, Trade and Industry, Japan. He holds 124 patents, has 21 publications in the control engineering field, more than 450 journal articles, and publications in conference proceedings. His research interests include controls and measurements. He is also interested in bio-measurement, sports science, robotics, fault diagnosis, vehicles, environmental monitoring, and intelligent control. He is a member of The Society of Instrument and Control Engineers.

• • •